Molecular Crystals and Liquid Crystals Science and Technology. Section A. Molecular Crystals and Liquid Crystals

Publication details, including instructions for authors and subscription information:
http://www.tandfonline.com/loi/gmcl19

Orientational Ordering of Domains in Vacuum-Grown Oligomer Thin Films: A Scanning Force Microscopy Study

F. Biscarini [a], O. Greco [a], A. Lauria [a], R. Zamboni [a] & C. Taliani [a]

[a] CNR-Istituto di Spettroscopia Molecolare, Via Gobetti 101, I-40129, Bologna, Italy

Version of record first published: 24 Sep 2006.

To cite this article: F. Biscarini , O. Greco , A. Lauria , R. Zamboni & C. Taliani (1996): Orientational Ordering of Domains in Vacuum-Grown Oligomer Thin Films: A Scanning Force Microscopy Study, Molecular Crystals and Liquid Crystals Science and Technology. Section A. Molecular Crystals and Liquid Crystals, 290:1, 203-212

To link to this article: http://dx.doi.org/10.1080/10587259608031906

Mol. Cryst. Liq. Cryst., 1996, Vol. 290, pp. 203–212
Reprints available directly from the publisher
Photocopying permitted by license only

ORIENTATIONAL ORDERING OF DOMAINS IN VACUUM-GROWN OLIGOMER THIN FILMS: A SCANNING FORCE MICROSCOPY STUDY

F. BISCARINI, O. GRECO, A. LAURIA, R. ZAMBONI, AND C. TALIANI
CNR-Istituto di Spettroscopia Molecolare, Via Gobetti 101, I-40129 Bologna, Italy

Abstract: We investigate by Scanning Force Microscopy the effects of the deposition temperature on the ordering of sexithienyl thin films grown on mica in high-vacuum. The low-temperature aggregates are formed by isotropic grains, while elongated lamellae appears, as the temperature increases which align along directions of the mica lattice. This change in the film morphology does not correspond to a discontinuity in the parameter which describes the anisotropy of the domains, while it makes the slope of the orientational order parameter (2nd Chebyshev polynomial) of the domains to change discontinuously. We infer that the transition is second-order or weak-first order, and we locate the corresponding transition temperature.

INTRODUCTION

α-sexithienyl (T6) is a π-conjugated molecule relevant to the studies of carrier and energy transport in organic thin films.[1] T6 is a prototype for the electronic properties of organic and polymer semiconductors. In addition, T6 is able to form aggregates in which molecules arrange into lamellae sheets as in a smectic phase,[2] and a nematic phase of T6 has also been observed.[3] This self-ordering, which arises from both the anisotropy and the strong intermolecular interactions, is of fundamental importance for understanding the intermolecular processes which are at the basis of the transport phenomena in molecular thin films. For instance, it has been reported that the hole mobility in field-effect transistors (FET)[4,5] with a T6 film as active layer increases from 5×10^{-4} to 0.02 $cm^2\ V^{-1}\ cm^{-1}$ as the molecular order increases.[5] The photoemission from light-emitting diodes (LED)[6] based on high-temperature grown T6 films is polarized. Since T6 films are grown in high-vacuum under non-equilibrium conditions, it is important to understand how the growth parameters control the film structure. In recent papers[7-9] we have shown with Scanning Force Microscopy (SFM) the quantitative aspects of the domain growth as a function of the deposition temperature. The domains grow according to an Arrhenius law with 0.36±0.04 eV activation energy. At each temperature, the domain size distribution is skewed towards large sizes, and both the mean value and the standard deviation decrease as the film gets thinner. Interestingly, the transition temperature from grains to lamellae depends on the film thickness.[7,8]

The aim of this paper is to discuss the evolution of the morphology towards strongly anisotropic thin films. In particular, we show that the onset of anisotropic domains within the film is continuous with the deposition temperature and we propose a method to locate the transition using the analysis of SFM images.

EXPERIMENTAL

Sample Preparation and SFM imaging

T6 was synthesized by coupling of the dimer via Grignard reagents catalyzed by Li.[10] The substrate is freshly cleaved ruby mica, which is a convenient model substrate due to its small corrugation. T6 films are grown in high - vacuum (HV) (base pressure $1x10^{-7}$ mbar) by sublimation of the purified material from a Knudsen cell placed 10 cm beneath the substrate and normal to it. The substrate effective temperature, which is the variable of our experiment, is calibrated with a thermo-resistor on the mica surface. The deposition rate is 0.2 - 1 Å/s, and the flow of material is shut when the nominal thickness reaches 100 nm. Our films are pale yellow in comparison with the dark yellow - orange ones investigated earlier [7] which were grown in a different setup. From the correlation length of the topographical features[9,11] of room temperature films with different thickness, we infer that our 100-nm samples are 3 times thinner than those studied earlier.[7] SFM images have been obtained in contact mode at 1-5 Hz scan rates. Soft silicon nitride cantilevers (spring constant 0.03 - 0.06 N/m) and a controlled atmosphere (relative humidity <20 %) have been used in order to avoid removal of material.

Statistical Analysis

We have applied the statistical procedure on SFM images described in ref. 7. Individual domains are selected from images of different scan size by drawing manually a 1-pixel rough boundary with a black line so that the boundary coincides with the lowest feature in the color scale. Then, thresholding is done within the manually drawn boundary at a slightly upper color, so that there is not necessarily alignment between the thresholding and the manually drawn data. However, we have chosen to work with the data from local thresholding to reduce the arbitrarity of the operator's judgement in following the optimal profile. Finally, we use NIH-IMAGE software (National Institute of Health, Bethesda, Maryland, USA) for pixel counting on the area obtained by thresholding at low height. In addition, other quantities such as the mean height, the length of the major and minor axis of the best-fit ellipsoid, and the angle α that the major axis forms with the fast scan

direction x are measured. We build statistical sets with N=400-500 domains and we estimate the average value of any property A as

$$\langle A \rangle = \frac{1}{N}\sum_{i=1}^{N} A_i . \qquad (1)$$

RESULTS AND DISCUSSION

Morphology and Structure

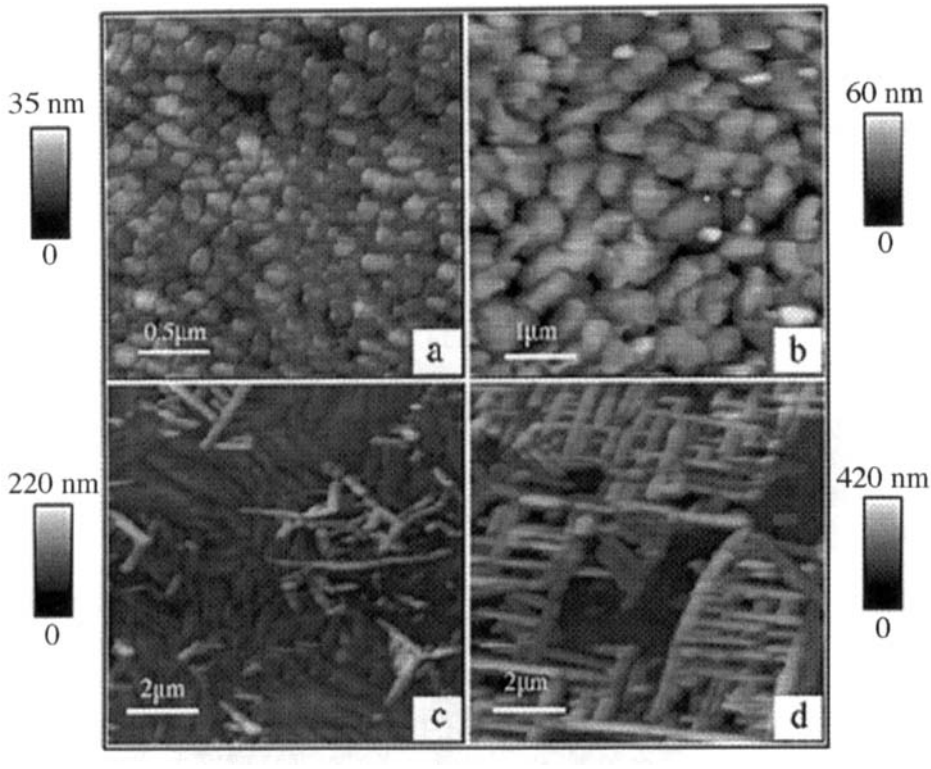

FIGURE 1. SFM topographical images of the morphology of 100-nm-thick T6 films grown on mica at a) 25° , b) 106 °, c) 130°, and d) 156°C.

The sequence in Fig. 1 shows the changes in the film morphology as a function of the deposition temperature. At room temperature (Fig. 1a) the film is made of spherical grains, suggesting isotropic aggregation or polymorphism. The latter might arise from the

coexistence of at least two distinct crystalline phases termed α and β, that have been revealed by low angle X-ray diffraction (XRD) on silicon.[2] These phases are originated by nucleation with the molecules standing (homeotropic) or lying flat (parallel arrangement) on the surface. As the deposition temperature increases to 106 °C the shape becomes slightly elongated (rice grains), and the grains seem to coalescence into larger domains separated by deep boundaries (Fig. 1b). This suggests the onset of an anisotropic growth, which is apparent in the higher temperature samples (Fig. 1c-d). At 130 °C a secondary nucleation of oriented lamellae start to form on the underlying grain texture. At 156 °C, a network of oriented lamellae is formed on large terraced domains (dark features in Fig. 1d), which are shown in Fig. 2 on a thinner film. The layered and ordered structure of this aggregate is evident from regularly-shaped *mesas* (features a in Fig. 2) that grow on top of larger islands (features b). The latter do not form a continuous film since they are separated by 6-7-nm-deep crevices (features c) with a flat bottom, presumably the mica substrate.

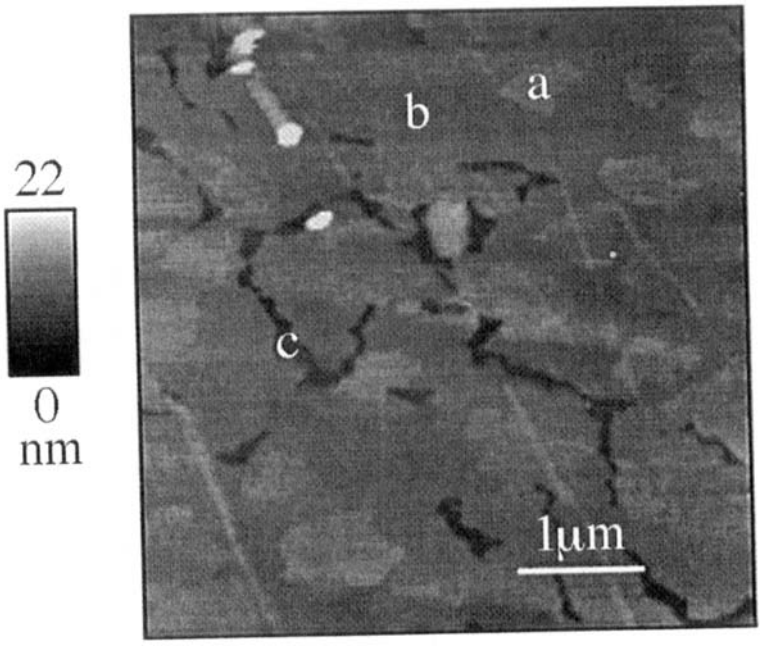

FIGURE 2. SFM image of a 5-nm-thick T6 film grown at 150°C on mica. Features labeled as a, b, and c are described in the text.

We measured the pixel-by-pixel mean height of the *mesas* and the islands on a 12 element set. Their height difference turns out to be 2.3±0.4 nm, which is in excellent agreement with the 2.24 nm interlayer spacing extracted from (l00) XRD peaks.[2] Thus, we infer that

in the films grown on mica at high temperature the molecules stand mostly upright with respect to the surface. The comparison between the terrace step and the van der Waals 2.7-nm-molecular length determined by Helium Atom Scattering [12] suggests that the long molecular axis is tilted by 31° with respect to the surface normal. This also indicates that the larger islands consist of 2-3 stacked molecular layers which might provide a well-ordered conduction plane at higher coverage. Our attempts to reproducibly image these films at higher lateral resolution were unsuccessful.

The results presented above show that the aggregation in T6 films evolve towards layered structures forming anisotropic domains and that these lamellae orient along preferential directions. We have exploited these features in order to assess the nature of this transition, as explained in the next section.

Evolution of the Anisotropy

For the i-th domain, we measure the anisotropy through the biaxial ratio $\mathcal{R}$:

$$\mathcal{R}_i = \frac{d_{\mathrm{maj},i} - d_{\mathrm{min},i}}{d_{\mathrm{maj},i} + d_{\mathrm{min},i}} , \qquad (2)$$

where d_{maj} and d_{min} are the lengths of the major and minor axes respectively of the best fit ellipsoid. The limit values $\mathcal{R} = 0$ and $\mathcal{R}=1$ imply perfectly isotropic and uniaxial domains respectively.

In Fig. 3 we show the evolution of the histograms with the deposition temperature for the samples imaged in Fig. 1. At room temperature the biaxial ratio is normally distributed with the average value $\langle\mathcal{R}\rangle\approx 0.1$, which indicates a negligible anisotropy of the grains. The "rice grain" aggregates at 106°C are characterized by a distribution skewed to the right. Its double-mode suggests the emergence of a second anisotropic population in addition to the dominant isotropic one. At 130°C the weights of the isotropic and anisotropic populations are equal, the distribution recovers the symmetry and its mode shifts to a value $\langle\mathcal{R}\rangle\approx 0.4$. At 156°C the lamellae prevail on the grains and there is a consequent shift of the mean value to $\langle\mathcal{R}\rangle\approx 0.6$.

The evolution of the mean value $\langle\mathcal{R}\rangle$ (not reported here) is almost linear with temperature and the transition from grains to lamellae takes place without any apparent discontinuity in the anisotropy parameter. Therefore, the parameter $\mathcal{R}$ turns out to be not a useful one for locating the transition temperature.

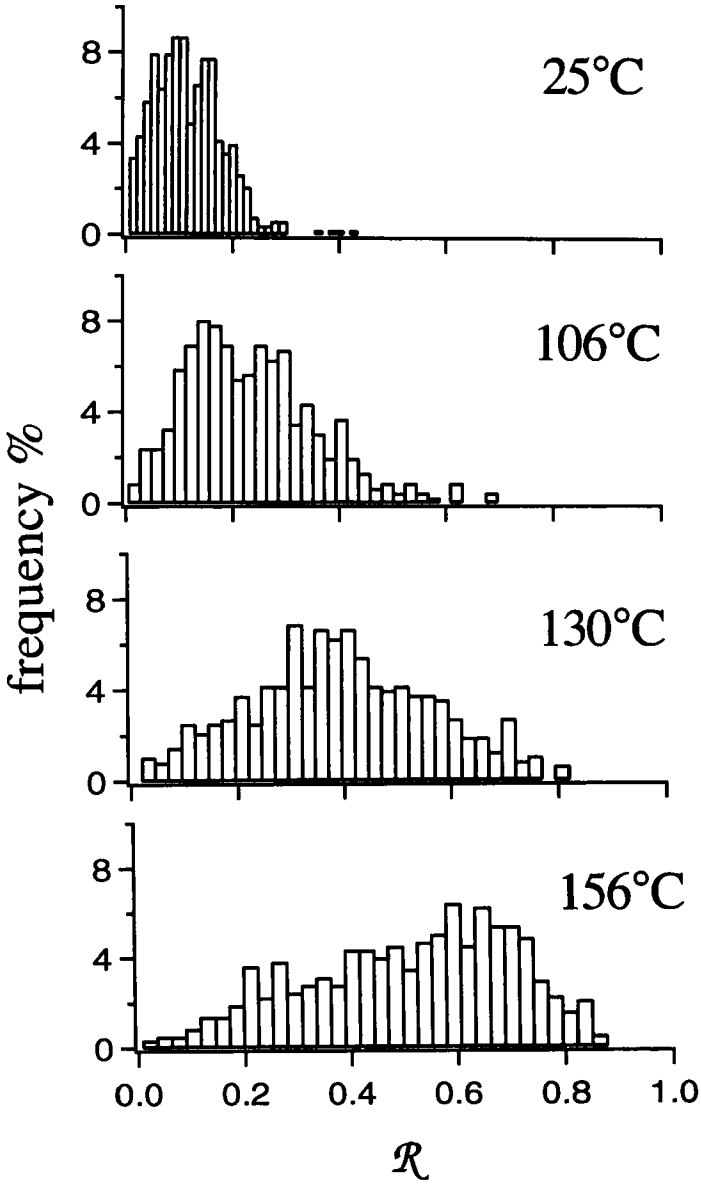

FIGURE 3. Distribution of the domain anisotropy $\mathcal{R}$ at different temperatures.

Orientational order parameter

The anisotropy might appear for two reasons. First, the crystal faces of the monoclinic $P2_1/n$[13] should grow at different rates. Second, as the deposition temperature increases the nucleation becomes favored mainly at kink sites of the anisotropic substrate. We perceive this to be the most important factor. Since the orthogonal extinction directions of mica coincide with the [100] and [010] crystallographic axes defining the basal plane, it is straightforward to observe under a polarizing microscope that most of the visible mica edges stretch along the extinction axes and at 60°, corresponding to the [110] and [110] directions. We find a similar distribution of orientations for the lamellae in the high-temperature aggregates, while we have not been able to observe any network of elongated lamellae in T6 films grown on amorphous quartz in the same batch.

The procedure that we have devised in order to quantify the orientational ordering of the domains is the following..First, we have measured the orientation of the major axis of the best fit ellipsoid of each domain. In order to evaluate meaningful averages of orientational functions it is necessary to know where to locate the physical reference frame, in such a way that only the relevant order parameters do not vanish when the system is ordered. The problem of measuring a preferred orientation in absence of an unambiguous laboratory frame such as an aligning field is encountered in Monte Carlo simulations of liquid crystal phases.[14] In that case the approach uses is to determine a suitable tensor in an arbitrary reference frame and then to diagonalize it.[15] The corresponding similarity tranformation rotates the tensorial properties to the physical reference frame. In our case, we keep the orientation of the sample with respect to the scan directions fixed and we acquire the images from distinct regions distant a few millimeters away, so that the weight of local features on the statistics diminishes. Then, we measure the azimuthal angle α between the major axis of each domain with the fast-scan direction x (xy frame), and we build a suitable order tensor whose elements are:

$$S_{ij} = \left\langle 2\cos\alpha_i \cos\alpha_j \right\rangle - \delta_{ij} . \tag{3}$$

Here the indices i and j run on the x and y scan directions, the average is performed as in eqn. (1), and δ_{ij} is Kronecker's delta. The 2x2 matrix S is the 2-D analogue of the Saupe ordering tensor, which is used to describe the orientations in a 3-D space.[15] When the matrix in eqn. 3 is diagonal (XY frame), the order parameter is given by:

$$S_{xx} = \langle \cos 2\alpha \rangle . \tag{4}$$

This is the second-rank Chebyshev polynomial which vanishes for an isotropic distribution of the major axis and is non-zero for a set of preferentially oriented domains on the surface.[16] The explicit expression for the order parameter (4) in terms of the angular functions in the *xy* frame follows from the diagonalization of the tensor (3):

$$S_{xx} = 2\sqrt{\langle\cos^2\alpha\rangle^2 - \langle\cos^2\alpha\rangle + \langle\cos\alpha\sin\alpha\rangle + 1/4}\,. \tag{5}$$

In Fig. 4 we plot the temperature behaviour of the order parameter S_{XX}. For grain aggregates S_{XX}. is virtually zero. For the lamellae, it is still zero at the onset of the transition, then rises almost linearly with temperature. Since no apparent discontinuity appears in the order parameter but a change of slope, we infer that the transition from grains to lamellae is either second-order or weak first-order. The transition temperature between grains and lamellae can be located as the intersection between the lines. In the case of these 100-nm thick films the transition occurs at about 120°C. It is interesting that for 300-nm films[7] the change was observed between 150°C and 200°C, while on 50-nm thick films it occurs between 75 and 100°C.[17]

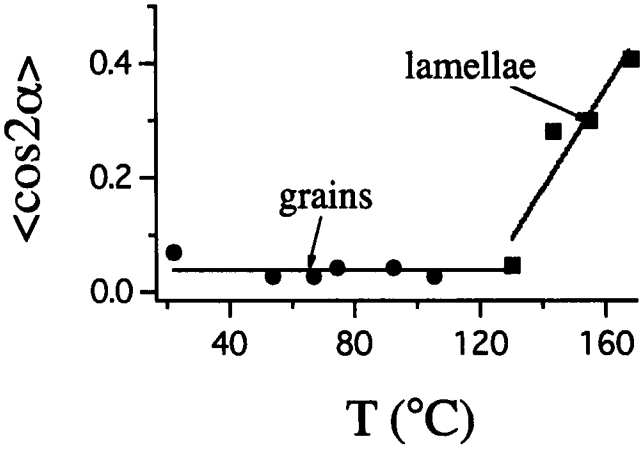

FIGURE 4. Orientational order parameter vs. temperature. Circles and squares are grains and lamellae, respectively. Straight lines represent best-fit for the lamellae data and mean value of the grain data, respectively.

Therefore, the transition temperature from grains to lamellae appears to depend on the film thickness and it is not an intrinsic property of the material. Such behaviour might be a due to a dimensionality effect, and it probably disappears above a critical thickness.

CONCLUSIONS

We have presented one of the first investigations of the character of a phase transition in organic thin films by means of SFM. T6 thin films grown at high-deposition temperature exhibit long-range order with anisotropic domains, as opposed to the usual isotropic/polycrystalline grain aggregates that have commonly been investigated. We have defined and measured from SFM images the shape anisotropy and an orientational order parameter (2nd Chebyshev polynomial). Their behaviour vs. temperature has allowed us to infer that the transition has a second or weak-first order character, and for 100-nm thick films we have located this transition at 120°C. Comparison with a recent study suggests that this transition temperature is a function of the film thickness (i.e. the amount of material deposited), so that this study might be relevant for the understanding of dimensionality effects (thin films vs. bulk materials) on the thermal behaviour.

ACKNOWLEDGEMENTS

We are grateful to V. Palermo, C. Zannoni, P. Samorì for useful suggestions and discussions. O. Greco and A. Lauria acknowledge EC Southern Italy research fellowships. Partial funding for this work was provided by EEC research programs Esprit Basic Research 8013 LEDFOS.

REFERENCES

1. S. Hotta and K. Waragai, Adv. Mater., 5, 896 (1993).
2. B. Servet, G. Horowitz, S. Ries, O. Lagorsse, P. Alnot, A. Yassar, F. Deloffre, P. Srivastava, R. Hajlaoui, P. Lang, and F. Garnier, Chem. Mat., 6, 1809 (1994).
3. (a) C. Taliani, R. Zamboni, G. Ruani, S. Rossini, and R. Lazzaroni, J. Mol. Electr. **6**, 225 (1990); (b) S. Destri, M. Mascherpa, and W. Porzio, Adv. Mat. **5**, 43 (1993).
4. G. Horowitz, X. Peng, D. Fichou, and F. Garnier, J. App. Phys, 67, 528 (1990).
5. A. Dodabalapur, L. Torsi, and H. E. Katz, Science, 268, 270 (1995).
6. R. N. Marks, F. Biscarini, R. Zamboni, and C. Taliani, Europhys. Lett., 32, 523 (1995).
7. F. Biscarini, R. Zamboni, P. Samorì, P. Ostoja, and C. Taliani, Phys. Rev., B52, 14868, (1995).
8. F. Biscarini, O. Greco, A. Lauria, P. Samorì, C. Taliani, and R. Zamboni, Polymer Preprints, in press (1996).

9. F. Biscarini, O. Greco, P. Samorì, and R. Zamboni, submitted (1996).
10. P. Ostoja, S. Guerri, M. Impronta, P. Zabberoni, R. Danieli, S. Rossini, C. Taliani, and R. Zamboni, Adv. Mat. Opt. Electr., 1, 127 (1992).
11. G. W. Collins, S. A. Letts, E. M. Fearon, . L. McEachern, and T. P. Bernat, Phys. Rev. Lett., 73, 2418 (1994).
12. M. Buongiorno Nardelli, D. Cvetko, V. De Renzi, L. Floreano, R. Gotter, A. Morgante, M. Peloi, F. Tommasini, R. Danieli, S. Rossini, C. Taliani, and R. Zamboni, Phys. Rev., B53, 1095 (1996).
13. (a) W. Porzio, S. Destri, M. Mascherpa, and S. Brückner, Acta Polymer., 44, 266 (1993); (b) G. Horowitz, B. Bachet, A. Yassar, P. Lang, F. Demanze, J-L. Fave, and F. Garnier, Chem. Mat., Adv. Mater., 7, 7(1995).
14. F. Biscarini, C. Chiccoli, P. Pasini, F. Semeria, and C. Zannoni, Phys. Rev. Lett., 75, 1803 (1995).
15. C. Zannoni, in The Molecular Physics of Liquid Crystals, edited by G. R. Luckhurst and G. W. Gray, (Academic Press, New York, 1979, Chap. 3, pp. 51-82.
16. V. Palermo, Laurea Thesis, University of Bologna (1995); V. Palermo, F. Biscarini, and C. Zannoni, unpublished (1996).
17. F. Biscarini, R. N. Marks, R. Zamboni, and C. Taliani, unpublished (1996).